

Poly(3,4-ethylenedithiathophene). A New Soluble Conductive Polythiophene Derivative

Chenggang Wang,[†] Jon L. Schindler,[‡] Carl R. Kannewurf,[‡] and
Mercuri G. Kanatzidis^{*,†,§}

Department of Chemistry and the Center for Fundamental Materials Research, Michigan State University, East Lansing, Michigan 48824, and Department of Electrical Engineering and Computer Science, Northwestern University, Evanston, Illinois 60208-3118

Received June 7, 1994. Revised Manuscript Received September 22, 1994[®]

A new polythiophene derivative has been synthesized by both chemical and electrochemical oxidative polymerization of the monomer 3,4-ethylenedithiathophene (EDTT). Both methods produce a polymer which is completely soluble in 1-methyl-2-pyrrolidinone (NMP) and partly soluble in tetrahydrofuran (THF) and chloroform. The FT-IR spectra of the neutral polymer indicate a regular structure formed via α,α coupling of thiophene rings. The new polymer shows two absorption bands at 341 nm and 413–419 nm in NMP solution in the UV–vis region. Photoexcitation of the polymer in dilute NMP solution results in a broad band luminescence with peak at ca. 552 nm. The redox behavior of the polymer was studied by cyclic voltammetry in 0.1 M (Bu₄N)ClO₄ acetonitrile solution. The average molecular weights have been determined by gel permeation chromatography (GPC) to be $M_n \sim 3.03 \times 10^3$ and $M_n \sim 4.75 \times 10^3$ for the chemically and electrochemically synthesized polymer, respectively. Electron spin resonance data are reported. Thermal gravimetric analysis studies show that the new polymer is stable in nitrogen up to 276 °C. The chemically doped (with FeCl₄⁻) polymer and the electrochemically doped (with ClO₄⁻) polymer show electrical conductivity of 0.1 and 0.4 S/cm at room temperature, respectively. These results are compared to some previously characterized polythiophenes.

Introduction

Polythiophenes and their derivatives have been investigated intensely because of their interesting electrical and electronic properties and relatively good environmental stability.¹ Significant experimental and theoretical effort² has been focused on the modification of their chemical structures, in order to alter their electronic structures and improve their electrical properties, environmental stability, and processability. For example, substituting long alkyl chains on the 3-position of thiophene affords a series of processable and highly conductive poly(3-alkylthiophenes).³ These properties

have been attributed to the higher solubility of polymers with long alkyl chains and suppression of unfavorable 2,4'-couplings that interrupt the conjugation system along the polymer backbone. Furthermore, using regiochemically defined oligothiophenes can lead to more regular conjugated polymers, due to the reduced number of 2,4-mislinkages.⁴ Fusing a benzene ring on the 3,4-position of thiophene leads to a low bandgap (1.0 eV) "transparent" conducting poly(isothianaphthene).⁵ This happens because the more stable planar quinoid form of the thiophene is favored with the presence of the benzene ring.⁶ Recently, the synthesis of nearly 100% head-to-tail poly(alkylthiophene) has been reported, which shows great improvement of conjugation chain length and high electrical conductivity.⁷ In addition to the numerous studies on poly(3-alkylthiophenes), polymers generated from 3,4-dialkylthiophene monomers also attracted considerable interest due to the fact that no possibility exists for α,β' or β,β' coupling of monomers during the polymerization process. This approach has

[†] Michigan State University.

[‡] Northwestern University

[§] A. P. Sloan Foundation Fellow 1991–93 and Camille and Henry Dreyfus Teacher Scholar 1993–95.

[®] Abstract published in *Advance ACS Abstracts*, November 1, 1994.

(1) For reviews, see: (a) Roncali, J. *Chem. Rev.* **1992**, *92*, 711–738. (b) Yamamoto, T. *Progr. Polym. Sci.* **1992**, *17*, 1153–1205. (c) Tourillon, G., Skotheim, T. J., Eds. *Handbook of Conducting Polymers*; Marcel Dekker: New York, 1986; Vol. I, pp 293–350. (d) Gustafsson, G.; Inganäs, O.; Salaneck, W. R.; Laasko, J.; Lopenon, M.; Taka, T.; Österholm, J.-E.; Stubb, H.; Hjertberg, T. In *Conjugated Polymers*; Bredas, J. L., Silbey, R., Eds.; Kluwer Academic Publishers: Netherlands, 1991; pp 315–362.

(2) Experimental: (a) Souto-Maior, R. M.; Hinkelmann, K.; Eckert, H.; Wudl, F. *Macromolecules* **1990**, *23*, 1268–1279. (b) Faid, K.; Cloutier, R.; Leclerc, M. *Macromolecules* **1993**, *26*, 2501–2507. (c) Roncali, J.; Gorgues, A.; Jubault, M. *Chem. Mater.* **1993**, *5*, 1456–1464. (d) Ritter, S. K.; Nofle, R. E.; Ward, A. E. *Chem. Mater.* **1993**, *5*, 752–754. (e) Yamamoto, T.; Sanechica, K.; Yamamoto, A. *J. Polym. Sci., Polym. Lett. Ed.* **1980**, *18*, 9–12. (f) Yamamoto, T.; Sanechica, K.; Yamamoto, A. *Bull. Chem. Soc. Jpn.* **1983**, *56*, 1503–1507. Theoretical: (a) Hong, S. Y.; Marynick, D. S. *Macromolecules* **1992**, *25*, 4652–4657. (b) Bredas, J. L.; Themans, B.; Andre, J. M.; Heeger, A. J.; Wudl, F. *Synth. Met.* **1985**, *11*, 343–352. (c) Otto, P.; Ladik, J. *Synth. Met.* **1990**, *15*, 327–335. (d) Quattrochi, C.; Lazzaroni, R.; Bredas, J. L.; Zamboni, R.; Taliani, C. *Macromolecules* **1993**, *26*, 1260–1264.

(3) (a) Hotta, S.; Rughooputh, S. D. D. V.; Heeger, A. J.; Wudl, F. *Macromolecules* **1987**, *20*, 212–215. (c) Leclerc, M.; Diza, F.; Wegner, G. *Makromol. Chem.* **1989**, *190*, 3105. (d) Sato, M.; Tanaka, S.; Kaeriyama, K. *J. Chem. Soc., Chem. Commun.* **1986**, 873–874.

(4) (a) Roncali, J.; Garnier, F.; Lemaire, M.; Garreau, R. *Synth. Met.* **1986**, *15*, 323–331. (b) Delabouglise, D.; Hmyene, M.; Horowitz, G.; Yassar, A.; Garnier, F. *Adv. Mater.* **1992**, *4*, 107–110.

(5) (a) Wudl, F.; Kobayashi, M.; Heeger, A. J. *J. Org. Chem.* **1984**, *49*, 3382–3384. (b) Kobayashi, M.; Colaneri, N.; Boysel, M.; Wudl, F.; Heeger, A. J. *J. Chem. Phys.* **1985**, *82*, 5717–5723.

(6) (a) Nayak, K.; Marynick, D. S. *Macromolecules* **1990**, *23*, 2237–2245. (b) Lee, Y. S.; Kertesz, M.; Elsenbaumer, R. L. *Chem. Mater.* **1990**, *2*, 526–530.

(7) (a) McCullough, R. D.; Lowe, R. D.; Jayaraman, M.; Anderson, D. L. *J. Org. Chem.* **1993**, *58*, 904–912. (b) McCullough, R. D.; Williams, S. P. *J. Am. Chem. Soc.* **1993**, *115*, 11608–11609. (c) McCullough, R. D.; Tristram-Nagle, S.; Williams, S. P.; Lowe, R. D.; Jayaraman, M. *J. Am. Chem. Soc.* **1993**, *115*, 4910–4911.

been drastically limited by the large steric hindrance of the two substituents,⁸ which forces the polymer backbone out of planarity and results in loss of conjugation and reduced electrical conductivity. Cyclization between 3,4 positions of thiophene considerably reduces the steric hindrance.⁹ Recently, we reported the synthesis and properties of the new polythiophene derivative poly(3',4'-dibutyl-2,2':5',2''-terthiophene) [poly(DBTT)],¹⁰ as another approach to reduce the steric hindrance and yield an ordered, soluble, conjugated polymer. In the poly(DBTT) backbone, every dibutyl-substituted thiophene unit is separated by two unsubstituted thiophene units (acting as steric diluents). The reduced number of side chains provides more space for the extension of the two butyl groups, minimizes extensive steric effects, and thus leads to a more coplanar conjugated polymer. In solution and in the solid state the poly(DBTT) appears to possess one of the longest chain conjugation lengths among polythiophenes.

Relative to monosubstituted polythiophenes, disubstituted polythiophenes are less well explored. To date, there have been only a few reports on the study of mercapto-substituted polythiophenes, in addition to alkyl, alkoxy and mixed alkyl, alkoxy disubstituted polythiophenes.¹¹ Poly[(3-methylmercapto)thiophene] (PMMT) has been prepared both chemically and electrochemically^{8a,12} and shows conductivity in the order of 10^{-1} – 10^{-2} S/cm. Poly[3-(ethylmercapto)thiophene] (PEMT) and poly[3,4-bis(ethylmercapto)thiophene] (PBE-MT) have been synthesized via a nickel-catalyzed Grignard coupling reaction of the corresponding 2,5-dihalogeno monomers.¹³ Both polymers are soluble in common organic solvents and semiconducting (10^{-3} and 10^{-7} S/cm, respectively) in the oxidized state. However, both the 3-(ethylmercapto)thiophene (EMT) and 3,4-bis(ethylmercapto)thiophene (BEMT) monomers fail to be electrochemically polymerized because neither monomer has significant positive spin density at both α -carbons on the thiophene rings according to the theoretical calculations.¹³ Recently, a new polythiophene derivative, poly(3,4-ethylenedioxythiophene) (PEDT), has been briefly reported.¹⁴ PEDT can be synthesized by either chemical or electrochemical polymerization of the corresponding 3,4-ethylenedioxythiophene (EDT) monomer and results in the conductivity of 15–19 and 200 S/cm, respectively. Unfortunately, PEDT is insoluble and infusible, which limits its further characterization. When a solution of the 3,4-ethylenedioxythiophene (EDT) monomer reacts with a thin layer of poly(vinyl acetate) containing an iron(III) salt, a transparent film

(1 μm thickness) of PEDT has been claimed to form. In this paper we report on the synthesis and characterization of the sulfur analog of PEDT, i.e., poly(3,4-ethylenedithiathiophene) [poly(EDTT)], which represents a new type of fused-ring mercapto-disubstituted polythiophene. In contrast to PEDT, the poly(EDTT) is completely soluble in NMP and partly soluble in THF, CHCl_3 , and other common organic solvents. This advantage lends this polymer to a more detailed spectroscopic, physicochemical, and charge-transport characterization than PEDT. The properties of poly(EDTT) are compared with some known related polythiophenes.

Experimental Section

1,2-Dibromoethane, *n*-butyllithium, carbon disulfide, and hydrazine hydrate were used as received from Aldrich Chemicals Inc. 3,4-Dibromothiophene was used as received from Lancaster Synthesis. Tetra-*n*-butylammonium perchlorate was purchased from GFS Chemicals Inc. and used without further purification. Acetonitrile (HPLC grade) and 1-methyl-2-pyrrolidinone (NMP) (HPLC grade) were used as received. Other solvents were distilled and degassed prior to use. All reactions were performed under an atmosphere of nitrogen or argon with either standard Schlenk or drybox techniques.

Thieno[3,4-*d*]-1,3-dithiole-2-thione. A solution of 3,4-dibromothiophene (4.95 g, 20.5 mmol) in anhydrous diethyl ether (30 mL) was cooled to -78°C (dry ice and acetone bath) under nitrogen. To this stirred precooled solution, *n*-butyllithium (8.2 mL, 20.5 mmol, 2.5 M in hexane) was added via syringe. The solution was stirred for 0.5 h, and then sulfur (0.66 g, 20.6 mmol) was added and stirred for 1 h. Another portion of *n*-butyllithium (8.2 mL, 20.5 mmol, 2.5 M in hexane) was added via syringe and stirred for another 0.5 h. To the reaction mixture, additional sulfur (0.66 g, 20.6 mmol) was added and stirred for an additional 1 h. Finally, the mixture was allowed to come to room temperature, and the solvent was removed under vacuum to get a yellow solid. To the yellow solid, 2 N sodium hydroxide solution (50 mL) and carbon disulfide (20 mL) were added. The mixture was refluxed under nitrogen for 6 h and then allowed to stand at room temperature overnight. The excess carbon disulfide was removed under vacuum, and the dark reaction mixture was filtered and washed with 2×30 mL of water to give a yellow solid. Recrystallization of the solid from dichloromethane–hexane (1:5 (v/v)) gave 0.85 g (22% yield) of thieno[3,4-*d*]-1,3-dithiole-2-thione as amber needles (lit.¹⁵ 33% yield); mp 142°C ; GC-MS (in ether solution) (*m/z*) (rel intensity) 190 (100), 146 (71.5), 126 (15.6), 82(10). ^1H NMR (CDCl_3) δ 7.21 (s, 2H).

3,4-Ethylenedithiathiophene (EDTT). Potassium metal (0.284 g, 7.28 mmol) was added in one portion into stirred, freshly distilled, methanol (75 mL) under nitrogen. After the potassium dissolved completely, thieno[3,4-*d*]-1,3-dithiole-2-thione (0.380 g, 2.0 mmol) was added to the solution. The reaction mixture was left to react for 1–2 h at 50°C under nitrogen, and gave a clear yellow solution. To this yellow solution, 1,2-dibromoethane (0.2 mL, 2.32 mmol) was added via syringe. After 24 h at room temperature, the methanol was removed under dynamic vacuum, and anhydrous ether (30 mL) was added. A yellow liquid of 3,4-ethylenedithiathiophene was obtained in 87.6% yield (0.305 g) when the ether was removed from the yellow filtered extract. GC-MS (*m/z*) (rel intensity) 174 (87), 159 (100), 146 (38), 82 (22). ^1H NMR (CDCl_3) δ 6.95 (s, 2H, aromatic), 3.21 (s, 4H, methylene). ^{13}C NMR (CDCl_3) δ 125.08 (aromatic, β -C), 118.06 (aromatic, α -C), 27.94 (methylene); FT-IR (KBr pellet) 3091(m), 2956(m), 2915(m), 1472(m), 1411(m), 1385(w), 1324(m), 1287(m), 857(s), and 772(s). UV–vis (CHCl_3) $\lambda_{\text{max}} = 283$ nm.

Poly(3,4-ethylenedithiathiophene) poly(EDTT)-C. Electrochemical Polymerization. Anhydrous FeCl_3 (0.57 g, 3.5 mmol) was dissolved in 80 mL of CH_3CN and stirred for 10 min. To this red-orange solution, a solution of 3,4-ethylene-

(8) (a) Gourillon, G.; Garnier, F. *J. Electroanal. Chem.* **1984**, *161*, 51–58. (b) Roncali, J.; Garreau, R.; Yassar, A.; Marque, P.; Garnier, F.; Lemaire, M. *J. Phys. Chem.* **1987**, *91*, 6706–6714.

(9) Roncali, J.; Garnier, F.; Garreau, R.; Lemaire, M. *J. Chem. Soc., Chem. Commun.* **1987**, 1500–1502.

(10) Wang, C.; Benz, M.; LeGoff, E.; Schindler, J. L.; Albritton-Thomas, J.; Kannewurf, C. R.; Kanatzidis, M. G. *Chem. Mater.* **1994**, *6*, 401–411.

(11) (a) Feldhues, M.; Kampf, G.; Litterer, H.; Mecklenburg, T.; Wegener, P. *Synth. Met.* **1989**, *28*, C487–C493. (b) Daoust, G.; Leclerc, M. *Macromolecules* **1991**, *24*, 455–459.

(12) (a) Elsenbaumer, R. L.; Jen, K. Y.; Oobodi, R. *Synth. Met.* **1986**, *15*, 169–174. (b) Tanaka, S.; Sato, M.; Kaeriyama, K. *Synth. Met.* **1988**, *25*, 277–288.

(13) (a) Ruiz, J. P.; Gleselman, M. B.; Nayak, K.; Marynick, D. S.; Reynolds, J. R. *Synth. Met.* **1989**, *28*, C481–C486. (b) Ruiz, J. P.; Nayak, K.; Marynick, D. S.; Reynolds, J. R. *Macromolecules* **1989**, *22*, 1231–1238. (c) Tasi, E. W.; Basak, S.; Ruiz, J. P.; Reynolds, J. R.; Rajeshwar, K. *J. Electrochem. Soc.* **1989**, *136*, 3683–3689.

(14) (a) Heywang, G.; Jonas, F. *Adv. Mater.* **1992**, *4*, 116–118. (b) Jonas, F.; Schrader, L. *Synth. Met.* **1991**, *41–43*, 831–836.

(15) Chiang, L.-Y.; Shu, P.; Holt, D.; Cowan, D. *J. Org. Chem.* **1983**, *48*, 4713–4714.

dithiathophene (0.15 g, 0.86 mmol) in 20 mL of CH₃CN was added dropwise. A dark-green precipitate formed immediately. The reaction mixture was stirred for about 24 h under nitrogen at room temperature. The dark-green solid was filtered through a glass frit and washed with 3 × 20 mL of fresh CH₃CN and dried under vacuum for 24 h. An amount of 0.076 g of product was obtained in doped form (~0.25 FeCl₄⁻ per repeat unit). The neutral form of the polymer was obtained by first Soxhlet extraction of the green solid with methanol, followed by acetone, and then treated with 20 mL of N₂H₄·H₂O for 12 h. The resultant mixture was filtered and Soxhlet-extracted again with methanol and then dried under vacuum for 12 h. Brown neutral poly(3,4-ethylenedithiathophene) [poly(EDTT)-C] was obtained in 43% yield (0.065 g). Elemental analysis by EDS showed almost no impurity of Fe and Cl (<0.5%). Calcd (%) for C₆H₄S₃: C 41.9; 2.30. Found (%): C 40.38; H 2.34.

The neutral polymer can be redoped by reaction with either 0.1 M FeCl₃/CH₃CN solution or 0.1 M I₂/CH₃CN solution. The solution-cast films (using NMP solution) can be doped with I₂ vapor in a closed chamber.

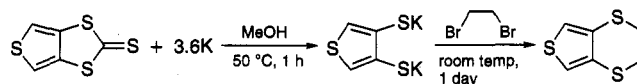
Poly(3,4-ethylenedithiathophene), poly(EDTT)-E. Electrochemical Polymerization. Electrochemical polymerization was carried out under potentiostatic conditions at the oxidation potential of the EDTT monomer ($E_{a,mon}$), at ambient temperature in a three-electrode single-compartment cell containing 5 mM monomer and 0.1 M (Bu₄N)ClO₄ in 20 mL of acetonitrile (HPLC grade, Aldrich). The working electrode was either a platinum disk electrode of 0.015 cm² area or a platinum plate electrode of 1.8 cm² area. The counter electrode was a platinum wire. A saturated calomel electrode (SCE) was used as the reference electrode. The solution was degassed by argon bubbling for 20 min prior to use and maintained under an argon blanket throughout each experiment. Thin films for electrochemical characterization were deposited on the small area platinum disk electrode at the oxidation potential of the EDTT for 1 min. The polymer-covered working electrode was then removed, washed with fresh acetonitrile, dried, and then transferred to another cell containing monomer-free 0.1 M (Bu₄N)ClO₄ acetonitrile solution for cyclic voltammetric analysis. Bulk doped polymer films were prepared on the larger area platinum plate electrode under the similar conditions by using ~20 mM (0.070 g) monomer in 0.1 M (Bu₄N)ClO₄ acetonitrile solution and holding at the oxidation potential of the EDTT for 45 min. After deposition, the films were rinsed with neat acetonitrile and dried under vacuum overnight. The doped polymer has ~0.33 ClO₄⁻ per repeat unit. Neutral (undoped) polymer poly(EDTT)-E were obtained by electrochemically reducing the doped films at -0.4 V/SCE until the residual cathodic current reached a constant value, then rinsed with neat acetonitrile, and were further chemically reduced by hydrazine hydrate under nitrogen for 12 h. They were washed with methanol, dried under vacuum overnight. Brown powder of neutral poly(3,4-ethylenedithiathophene) [poly(EDTT)-E] was obtained in 13% yield (0.009 g). EDS showed no chloride impurity. Calcd (%) for C₆H₄S₃: C 41.9; 2.30. Found (%): C, 39.80; H, 2.75.

Instrumentation. Elemental analyses (semiquantitative) were performed on a JEOL JSM-35C scanning electron microscope (SEM) equipped with a Tracor Northern energy-dispersive spectroscopy (EDS) detector. Infrared spectra were recorded as KBr pressed pellets on a Nicolet 740 FT-IR spectrometer. Carbon and hydrogen elemental analyses were performed by Oneida Research Services Inc., Whitesboro, NY. UV-visible-NIR absorption spectra were obtained from a Shimadzu UV-3101PC double-beam, double-monochromator spectrophotometer. Nuclear magnetic resonance spectra (¹H and ¹³C) were obtained using a computer-controlled Varian Gemini NMR (300 MHz) spectrometer. The chemical shifts are reported in parts per million (δ , ppm) using the residual solvent resonance peak as reference (CHCl₃, δ 7.24 ppm for ¹H and 77.0 ppm for ¹³C). Fluorescence emission and excitation spectra were measured on a Perkin-Elmer LS-5 fluorescence spectrophotometer. Thermogravimetric analysis (TGA) and differential scanning calorimetry (DSC) were performed on Shimadzu TGA-50 and DSC-50 under nitrogen or oxygen at 5 °C/min heating rate. Electron spin resonance (ESR)

spectra were recorded with a Varian EPR-E4 spectrometer with diphenylpicrylhydrazyl radical as *g* marker ($g = 2.0037$). Cylindrical quartz tubes were employed for powders. The conductivity data were measured by the standard four-probe method on pressed pellets as a function of temperature as described elsewhere.¹⁶ The molecular weight of the poly(EDTT)-C and poly(EDTT)-E was estimated by gel permeation chromatography (GPC) (relative to polystyrene standards, M_w in the range 3120–500 800) with Shimadzu LC-10AS liquid chromatograph equipped with a PL-GEL 10u (MIXED-B) column of length 300 mm, using 1-methyl-2-pyrrolidinone (NMP) with and without containing 0.5 wt % LiCl as an eluent. Electrochemical polymerization and cyclic voltammetry were performed with a PAR 273 potentiostat/galvanostat equipped with a PAR RE0091 X-Y recorder.

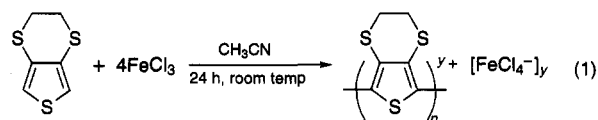
Results and Discussion

Monomer Synthesis. The precursor thieno[3,4-*d*]-1,3-dithiole-2-thione was prepared from 3,4-dibromothiophene using a slightly modified procedure reported by Chiang et al.¹⁵ Potassium reacts with the thione in methanol to form the dipotassium salt intermediate via the C–S bond cleavage. The dipotassium salt of the thiophene–dithiolate intermediate (**2**) reacts with dibromoethane to give the new monomer 3,4-ethylenedithiathophene (EDTT) in good yield (87.6%), as shown here:



The structure and purity of the monomer were confirmed by FT-IR, ¹H NMR, and ¹³C NMR results as described in the Experimental Section.

Oxidative Polymerization. Both chemical and electrochemical methods have been used in the oxidative polymerization of aromatic heterocycles.¹⁷ To distinguish the origin of the polymer, we will use the designations poly(EDTT)-C and poly(EDTT)-E for the chemically and electrochemically prepared material, respectively. For chemical polymerization we used FeCl₃ as a convenient oxidant to polymerize EDTT, followed by reduction with hydrazine hydrate (N₂H₄·H₂O) to obtain the undoped polymer (eq 1).



To determine the proper conditions for electropolymerization, we first examined the cyclic voltammetry (CV) of the EDTT monomer. During the first anodic scan, a solution of EDTT exhibited a rapid increase in current at the electrode with an onset of 1.15 V vs SCE as illustrated in Figure 1A. Application of repetitive potential scans (between 0.0 and 1.2 V vs SCE) to the monomer solution resulted in a new anodic process well

(16) (a) Lyding, J. W.; Marcy, H. O.; Marks, T. J.; Kannewurf, C. R. *IEEE Trans. Instrum. Meas.* **1988**, *37*, 76–80. (b) Marcy, H. O.; Marks, T. J.; Kannewurf, C. R. *IEEE Trans. Instrum. Meas.* **1990**, *39*, 756–760.

(17) (a) E. Waltman, R. T.; Bargon, J.; Diaz, A. F. *J. Phys. Chem.* **1983**, *87*, 1459–1463. (b) Yoshino, K.; Nakajima, S.; Sugimoto, R. *Jpn. J. Appl. Phys.* **1987**, *26*, L1038–L1039. (c) Hotta, S.; Soga, M.; Sonoda, N. *Synth. Met.* **1988**, *26*, 267–279.

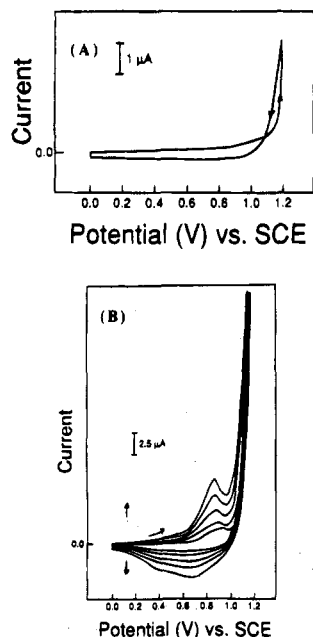


Figure 1. Cyclic voltammogram of 3,4-ethylenedithiathophene (EDTT) monomer (5 mM) in $\text{CH}_3\text{CN}/0.1 \text{ M } (\text{Bu}_4\text{N})\text{ClO}_4$ on a Pt disk electrode. Scan rate, 100 mV/s. (a) First scan showing nucleation loop on the Pt electrode. (B) Fourth to eighth scan showing polymer deposition on the Pt electrode.

below the onset of oxidation of the monomer. The intensity of this new anodic process (at $\sim 0.91 \text{ V}$ vs SCE, scanning at 100 mV/s) increases, as shown in Figure 1B. This is consistent with conducting polymer deposition on the anode surface and is confirmed by the formation of small amount of dark-green deposit on the electrode. The oxidation potential of the EDTT monomer is $E_{a,\text{mon}} = 1.15 \text{ V}$ vs SCE which is lower than that of thiophene (T, $E_{a,\text{mon}} = 1.65 \text{ V/SCE}$) and 3-(methylmercapto)thiophene (MMT, $E_{a,\text{mon}} = 1.30 \text{ V/SCE}$).^{8a} The trend in oxidation potentials is consistent with the presence of two electron-donating sulfur atoms on the β positions of the thiophene ring. The low oxidation potential of the EDTT monomer demonstrates the ease of formation of the radical cations and suggests polymerization will occur with fewer side reactions. Two of the possible side reactions avoided here include the formation of β linkages and overoxidation of the polymer. By holding the working electrode potential at 1.15 V/SCE for 0.5 h, a thick dark-green, smooth deposit was obtained which could not be peeled off as a free-standing film because of its somewhat brittle nature. By stripping off the outer layer with adhesive tape, it was possible to measure the electrical conductivity of the polymer. A pressed pellet was used for the four-probe variable-temperature electrical conductivity measurements (see below).

The successful oxidative polymerization of the EDTT monomer stands in contrast to EMT and BEMT which cannot polymerize under the same conditions.¹³ On the basis of the spin density argument advanced for EMT and BEMT radical cations, it can be concluded that in the EDTT radical cation, the positive spin density is mainly localized on both α positions of the thiophene ring. Theoretical calculations of the cation-radical spin densities for the EDTT monomer are needed, however, to confirm this.

Regardless of the polymerization method, poly(EDTT) is completely soluble in NMP and partly soluble in THF

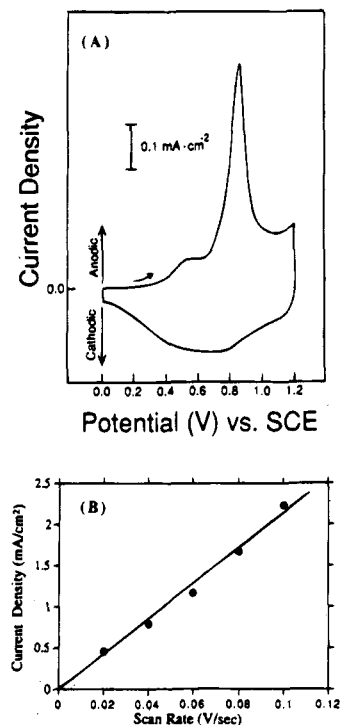


Figure 2. (A) Typical cyclic voltammogram of a directly electrogenerated poly(EDTT)-E film on Pt electrode in $\text{CH}_3\text{CN}/0.1 \text{ M } (\text{Bu}_4\text{N})\text{ClO}_4$. Scan rate, 20 mV/s. (B) Plot of peak current density vs the scan rate for a directly electrogenerated poly(EDTT)-E film on Pt electrode in $\text{CH}_3\text{CN}/0.1 \text{ M } (\text{Bu}_4\text{N})\text{ClO}_4$.

and CHCl_3 . This is in contrast to its oxygen analog, PEDT, which is totally insoluble. The solubility of poly(EDTT) allows us to do a detailed spectroscopic characterization of this new polythiophene derivative. The powder X-ray diffraction (XRD) pattern of the neutral poly(EDTT)-C shows that it is amorphous.

Polymer Electrochemistry. The electrochemistry of both poly(EDTT)-C and poly(EDTT)-E was studied by cyclic voltammetry. Figure 2A shows a representative cyclic voltammogram (CV) of a directly electrogenerated poly(EDTT)-E film on a Pt electrode in 0.1 M $\text{Bu}_4\text{NClO}_4/\text{CH}_3\text{CN}$ solution at scan rate of 20 mV/s. The E_{pa} and E_{pc} values are linearly dependent on scan rate. The CV of electrogenerated poly(EDTT)-E exhibits a broad, weak, first anodic peak at +0.54 V/SCE and a sharp strong second anodic peak at +0.86 V vs SCE. The latter is associated with one broad cathodic peak at ca. +0.70 V/SCE. These two oxidation steps seem to be related to the formation of polarons and bipolarons, as has been seen in several polythiophene derivatives.¹⁸ The high symmetry and narrowness of the second anodic peak (half-height width = 84 mV) suggests relatively homogeneous conjugated chains. The second anodic peak currents vary linearly with scan rates in the range 0.02–0.1 V/s as shown in Figure 2B, which indicate the surface-confined nature of the species, as has been observed in many polythiophenes.¹⁹ No significant loss of electroactivity was seen after 50 cycles as the applied potential swept continuously between 0.0

(18) (a) Zotti, G.; Schiavon, G. *Synth. Met.* **1989**, *31*, 347–357. (b) Child, A. D.; Reynolds, J. R. *J. Chem. Soc., Chem. Commun.* **1991**, 1779–1781. (c) Guay, J.; Kasai, P.; Diaz, A.; Wu, R.; Tour, J. M. *Chem. Mater.* **1992**, *4*, 1097–1105.

(19) Tourillon, G.; Garnier, F. *J. Electroanal. Chem.* **1984**, *161*, 51–58.

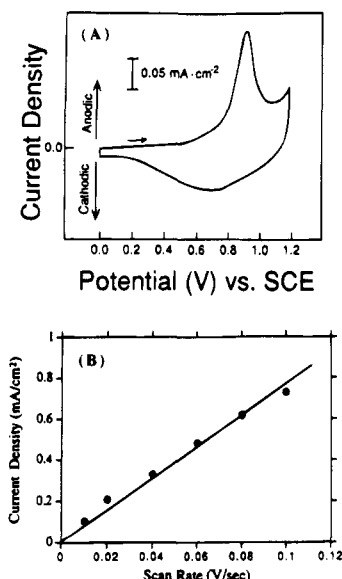


Figure 3. (A) Typical cyclic voltammogram of a cast poly(EDTT)-C film on Pt electrode in $\text{CH}_3\text{CN}/0.1 \text{ M } (\text{Bu}_4\text{N})\text{ClO}_4$. Scan rate, 20 mV/s. (B) Plot of peak current density vs the scan rate for a cast poly(EDTT)-C film on Pt electrode in $\text{CH}_3\text{CN}/0.1 \text{ M } (\text{Bu}_4\text{N})\text{ClO}_4$.

and 1.2 V vs SCE. The film was brown-yellow in the neutral state and dark-green in the oxidized state.

For comparison, the electrochemical behavior of the chemically synthesized poly(EDTT)-C in the solid state was also investigated with solution-cast films (NMP solution) on a Pt electrode. Figure 3A shows a representative cyclic voltammogram of a cast film of poly(EDTT)-C. It exhibits a reversible redox process with an anodic peak potential (E_{pa}) at 0.92 V and a cathodic peak potential (E_{pc}) at 0.69 V vs SCE and at 20 mV/s. The anodic peak is noticeably sharper than the cathodic peak and the narrow peak width at half-height of about 84 mV indicates a homogeneous and relatively narrow distribution of conjugation lengths among the polymer chains. This is in agreement with the relatively small polydispersity found from the GPC molecular weight measurements (see below). A large potential hysteresis ($\Delta E_p = 0.23 \text{ V}$) is attributed to a number of factors including the ease of diffusion of dopant ions in and out of the film, film thickness, and conformational relaxation of polymer chains between the rigid planar oxidized and flexible neutral states. The film was brown-yellow in the neutral state and dark-green in the oxidized state. No significant loss of electroactivity was seen after 30 cycles. The peak currents vary linearly with scan rate (see Figure 3B), as was observed in the electrochemically prepared polymer. We also observe that the E_{pc} is relatively independent of scan rate, while the E_{pa} shifts to higher positive values with increased scan rates.

The cyclic voltammetry of poly(EDTT)-C differs slightly from that of poly(EDTT)-E, in that the first anodic redox wave occurs at a slightly higher oxidation potential, suggesting smaller average molecular weight for poly(EDTT)-C relative to poly(EDTT)-E. Thus, as has been found in other conjugated polymers,²⁰ the method of synthesis yields a slightly different polymer. Both the oxidation potentials of poly(EDTT)-C ($E_{pa} = 1.00 \text{ V/SCE}$)

and poly(EDTT)-E ($E_{pa} = 0.90 \text{ V/SCE}$) are lower than those of PBEMT ($E_{pa} = 1.27 \text{ V/SCE}$) but comparable to PEMT ($E_{pa} = 0.98 \text{ V/SCE}$).¹³

Chromatographic Molecular Weight Studies.

The average molecular weights of both poly(EDTT)-C and poly(EDTT)-E were determined by gel permeation chromatography (GPC). The molecular weights were estimated from a retention time calibration curve constructed using a series of polystyrene standards. This commonly used technique assumes that, in solution, the conjugated polymer and polystyrene behave similarly, which we recognize may not be entirely appropriate. Thus, the numbers reported here are only relative. Both neat NMP and NMP containing $\sim 0.5 \text{ wt } \% \text{ LiCl}$ were used as eluents with a flow rate of 0.2 mL/min. The UV-vis detector was set at 400 nm with a temperature of 23 °C. A dramatic difference in the GPC results is observed when $\sim 0.5 \text{ wt } \% \text{ LiCl}$ is added to the NMP solvent. In the absence of LiCl, a multimodal distribution of polymer species was observed in the GPC trace corresponding to very high molecular weights. When LiCl is added to the solution, this behavior disappears and only one peak is observed. For example, a representative GPC trace of the poly(EDTT)-C is presented in Figure 4, where the molecular weight distribution is clearly trimodal in character in neat NMP. It basically consists of a high and a low molecular weight fraction with area of ca. 38% and 62%, respectively. The high molecular weight fraction corresponds to number average molecular weight (M_n) $\sim 3.93 \times 10^5$ and weight average molecular weight (M_w) $\sim 5.30 \times 10^5$ with polydispersity (PD) of 1.35 and is due to polymer chain aggregates in solution. The low molecular weight fraction corresponds to $M_n \sim 2.64 \times 10^3$ and $M_w \sim 5.38 \times 10^3$ with PD of 2.0. Figure 4B shows the single peak obtained when the NMP/0.5 wt % LiCl was used as an eluent. This peak has a longer retention time and corresponds to a molecular weight fraction ($M_n = 3.03 \times 10^3$, $M_w = 5.75 \times 10^3$, PD = 1.9). The dramatic change in the GPC trace upon addition of LiCl suggests that in neat NMP the polymer does not disperse into single chains but forms intermolecular aggregates, which give rise to the large molecular weight. Li^+ ions help dissolve these aggregates, probably via Lewis acid-base interactions, into single chains and allows for the estimation of the correct molecular weight. Such aggregation phenomena in NMP have been observed in previous GPC studies of polyanilines.²¹ Similar behavior was observed in the GPC measurements of the poly(EDTT)-E. A single GPC trace was observed, corresponding to the $M_n = 4.75 \times 10^3$, $M_w = 8.08 \times 10^3$, PD = 1.7, when NMP/0.5 wt % LiCl was used as an eluent (see Figure 4C,D).

In comparison with poly(3-ethylmercapto)thiophene (PEMT)¹³ ($M_n = 2200$, $M_w = 13000$, DP = 5.9), and poly[3,4-bis(ethylmercapto)thiophene (PBEMT)] ($M_n = 2600$, $M_w = 9000$, DP = 3.46), the M_n of poly(EDTT)-C and poly(EDTT)-E are slightly higher, though in the same order of magnitude. The M_n corresponds to about 17 repeat units in the polymer chain for poly(EDTT)-C and 27 repeat units for poly(EDTT)-E. The relatively small polydispersity indexes for both poly(EDTT)-C and

(20) Shi, L. H.; Garnier, F.; Roncali, J. *Macromolecules* **1992**, *25*, 6425–6429.

(21) (a) Hsu, C.-H.; Peacock, P. M.; Flippen, R. B.; Manohar, S. K.; MacDiarmid, A. G. *Synth. Met.* **1993**, *60*, 233–237. (b) Wei, Y.; Hariharan, R.; Patel, S. A. *Macromolecules* **1990**, *23*, 758–764.

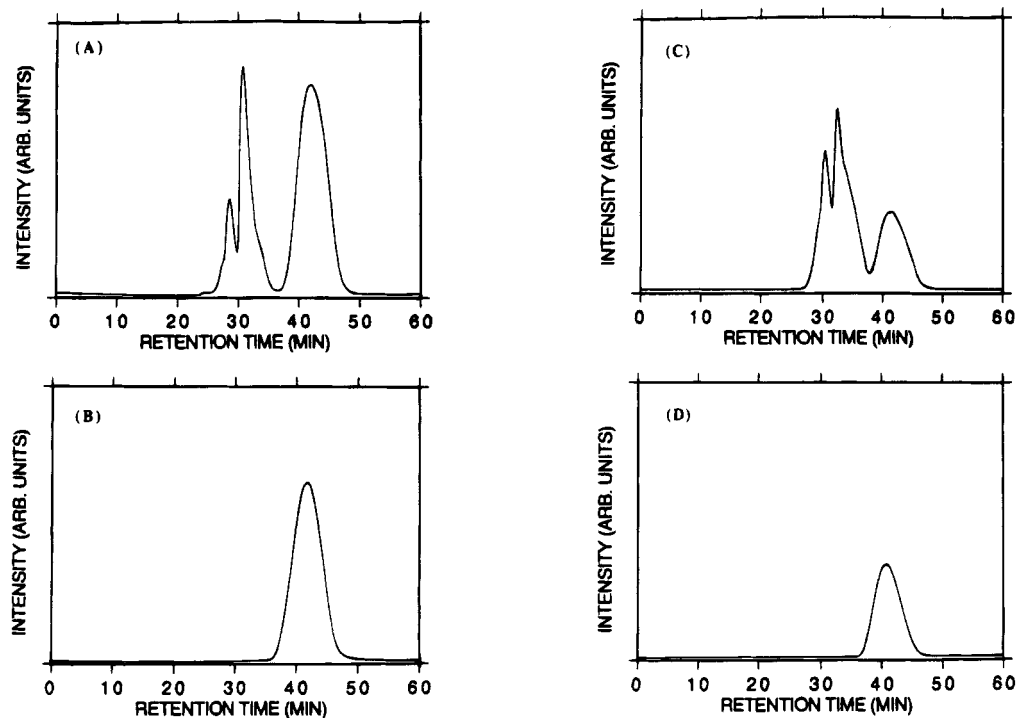


Figure 4. GPC traces of neutral poly(3,4-ethylenedithiathophene) in NMP solution at room temperature. (A) poly(EDTT)-C, without LiCl, (B) poly(EDTT)-C, with addition of LiCl (C) poly(EDTT)-E, without LiCl (D) poly(EDTT)-E, with addition of LiCl. The Li^+ ions are thought to serve as Lewis acid centers probably complexing the sulfur atoms on the polymer chains, interfering with chain-to-chain interactions. Thus, they help dissolve the large agglomerated particles into single chains.

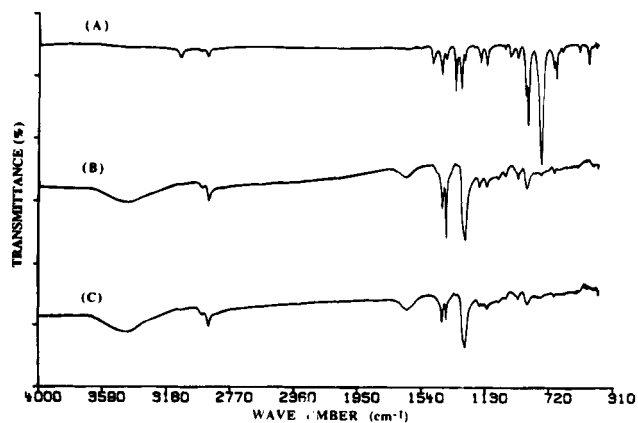


Figure 5. FT-IR transmission spectra (KBr pellets) of (A) monomer 3,4-ethylenedithiathophene (EDTT), (B) neutral poly(EDTT)-C, and (C) neutral poly(EDTT)-E.

poly(EDTT)-E indicate a more homogeneous distribution of polymer chain lengths.

Infrared Spectroscopy. Figure 5 shows the infrared spectra of the EDTT monomer and the corresponding neutral polymers poly(EDTT)-C and poly(EDTT)-E. The principal IR absorption bands for the monomer and polymer and their assignments, including data for mono- and poly-(3-ethylmercapto)thiophene (EMT and PEMT), mono- and poly-[3,4-bis(ethylmercapto)thiophene (BEMT and PBEMT), poly(3',4'-dibutyl-2,2':5',2''-terthiophene) [poly(DBTT)], polythiophene (PT), and poly(3-hexylthiophene) (P3HT) are compared in Table 1. The absence of absorbance at 820 cm^{-1} (due to $\text{C}_\beta\text{-H}$ bending vibration) in the spectra of PBEMT, poly(EDTT)-C, and poly(EDTT)-E is consistent with the lack of thiophene ring hydrogen atoms in these polymers. In the thiophene ring vibration region, only two peaks are present in the EDTT monomer and the poly(EDTT)-C. The reduced number of vibrational modes, compared to

the other listed polymers, could be attributed to the existence of additional symmetry in the chemical structure of the repeating units. Similar effects were observed in the IR spectra of poly(DBTT).¹⁰ The absence of the aromatic $\text{C}_\beta\text{-H}$ stretch at 3070 cm^{-1} is consistent with the 3,4-disubstitution in the monomer and in the corresponding polymers. The band due to $\text{C}_\alpha\text{-H}$ stretch at ca. 3091 cm^{-1} is nearly absent in the IR spectra of poly(EDTT)-C and poly(EDTT)-E in contrast to the IR spectra of PEMT and PBEMT, and this can be attributed to the higher molecular weights for the poly(EDTT)-C and poly(EDTT)-E, in agreement with the GPC results. However, there are slight differences in the IR spectra of poly(EDTT)-E and poly(EDTT)-C. This may be because the two different synthetic methods yield products which may differ in the degree of crystallinity, cis/trans conformation ratio, and the number of defects.

The IR spectra of the oxidized polymer, doped with FeCl_4^- , I_3^- (chemically), and ClO_4^- (electrochemically), are all similar and shown in Figure 6. The doping process causes a profound change in the IR spectra presumably due to the change in the electronic structure of the neutral polymer. Surprisingly, the doped polymers (regardless of the dopant anion) have an additional intense band at $831\text{--}818\text{ cm}^{-1}$. In other polythiophene derivatives, this band has been assigned to the $\text{C}_\beta\text{-H}$ deformation vibration of the 2,3,5-trisubstituted thiophene ring.²² However, in the polymers described here such a $\text{C}_\beta\text{-H}$ group does not exist. We note that this band is not observed in the IR spectrum of the neutral polymer and it disappears when the doped polymers are reduced back to the undoped state. This precludes the possibility of a C-S cleavage and formation of a C-H group on the thiophene ring upon doping. Thus, the

Table 1. Comparison of Infrared Band Positions (cm^{-1}) and Their Assignments for Some Monomeric and Polymeric Polythiophene Derivatives^a

sample	arom C-H		aliph C-H stretch	ring stretch	methyl def		arom C-H out-of-plane					
	α	β										
EDTT	3091		2956	2915	1472	1411	1385	970	857	772		
poly(EDTT)-C			2951	2911	1442	1409	1384					
poly(EDTT)-E			2962	2909		1409	1373					
EMT ^b	3101	3066	2974	2924	2870	1492	1446	1427	1373	1099	852	779
PEMT ^b	3090	3070	2974	2916	2867	1508	1481	1423	1373		825	
BEMT ^b	3101		2970	2924	2870	1473	1446	1427	1373	960	856	787
PBEMT ^b	3090		2968	2922	2865	1508	1489	1446	1373			
poly(DBTT) ^c		3062	2951	2925	2856	1492	1456		1377		788	
PTH ^d		3063				1491	1453	1441	1377		788	
P3HT ^d		3055	2959	2930	2858	1512	1458	1439	1377		825	

^a All polymers are in the undoped state. ^b See ref 13. ^c See ref 10. ^d See ref 3a PTH-polythiophene, P3HT-poly(3-hexylthiophene).

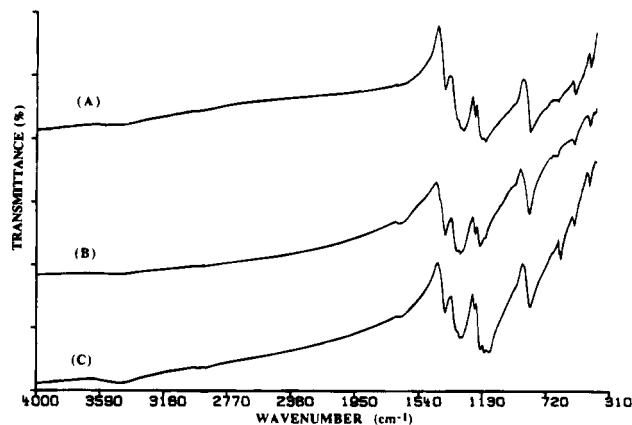


Figure 6. FT-IR transmission spectra (KBr pellets) of (A) poly(EDTT)-C doped with FeCl_4^- , (B) poly(EDTT)-C doped with I_3^- , and (C) poly(EDTT)-E doped with ClO_4^- .

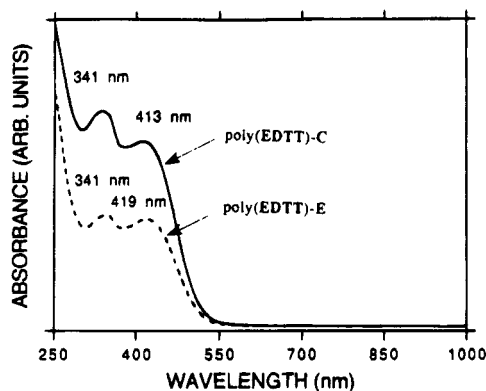


Figure 7. UV-visible absorption spectra of poly(EDTT)-C and poly(EDTT)-E in NMP solution at room temperature.

origin of this band is uncertain at this stage. The bands at 1110 and 625 cm^{-1} in Figure 6C are due to the presence of ClO_4^- dopant. The higher background absorbance levels at the high-energy region of the spectra, compared to the undoped polymer, are characteristic of conducting polymers and is attributed to the tailing of the electronic bipolaronic absorption from oxidatively doped regions in the polymer.

UV-Vis-NIR Spectroscopy. The electronic spectra of both poly(EDTT)-C and poly(EDTT)-E in NMP solution display two absorption bands in the UV-vis region as shown in Figure 7, in contrast to the single absorption observed in the case of PEMT and PBEMT and some other polythiophenes. The low-energy peaks, both with an onset around 2.39 eV (518 nm), have an absorption maximum at 413 nm for poly(EDTT)-C and 419 nm for poly(EDTT)-E, which is a result of the $\pi-\pi^*$

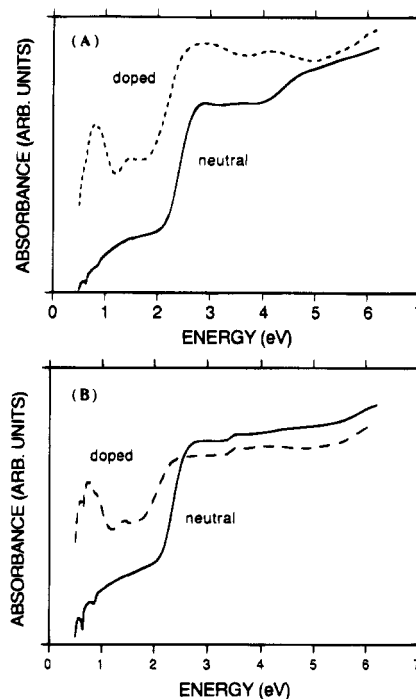


Figure 8. UV-visible-NIR absorption spectra of (A) neutral and doped poly(EDTT)-C films and (B) neutral and doped poly(EDTT)-E films at room temperature.

absorption transition.²³ The higher energy peaks at 341 nm are attributed to $n-\pi^*$ transitions involving the excitation of nonbonding electrons from the periphery substituents (i.e., S atoms) to the antibonding π^* orbitals of the heterocyclic rings. The onset of UV-vis absorption in poly(EDTT)-C and poly(EDTT)-E, in solution, is close to that of PBEMT (2.4 eV) but slightly larger than that of PEMT (2.2 eV), suggesting enhanced ring rotation in poly(EDTT).

Figure 8A shows electronic spectra of neutral and doped solid films of poly(EDTT)-C. In the solid state, the absorption maximum of poly(EDTT)-C appears at 434 nm, indicating a greater degree of planarity than in solution.²⁴ The bandgap of the poly(EDTT)-C of ca. 2.19 eV (onset of the $\pi-\pi^*$ transition), which is also confirmed by optical diffuse reflectance measurements, lies between that of PEMT ($E_g \sim 2.0\text{ eV}$) and PBEMT ($E_g \sim 2.24\text{ eV}$). Upon doping with iodine vapor, the doped solid film shows two new low-energy absorptions

(23) (a) Rughooputh, S. D. D. V.; Hotta, S.; Heeger, A. J.; Wudl, F. *J. Polym. Soc., Polym. Phys. Ed.* **1987**, *25*, 1071-1078. (b) Curtis, R. F.; Phillips, G. T. *Tetrahedron* **1967**, *23*, 4419-4424.

(24) Inganas, O.; Salaneck, W. R.; Osterholm, J.-E.; Laakso, J. *Synth. Met.* **1988**, *22*, 395-406.

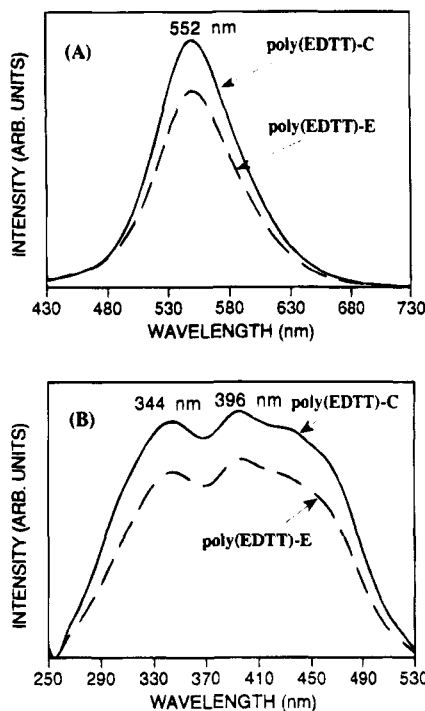


Figure 9. (A) Fluorescence emission spectra of poly(EDTT)-C and poly(EDTT)-E in dilute NMP solution at room temperature ($\lambda_{\text{ex}} = 400$ nm) and (B) excitation spectra of poly(EDTT)-C and poly(EDTT)-E in dilute NMP solution at room temperature.

with peak maxima at ~ 0.80 and 1.47 eV. This is qualitatively similar to other polythiophenes and consistent with charge storage primarily in bipolarons.²⁵ The electronic spectra of cast films (from NMP solution) of poly(EDTT)-E in the neutral and doped state show similar features to those of poly(EDTT)-C, as depicted in Figure 8B. The bandgap of the poly(EDTT)-E is slightly lower at ~ 2.14 eV. Upon doping with iodine vapor, the doped solid film shows two new lower energy absorptions with peak maxima at ~ 0.74 and 1.41 eV. These results are consistent with the slightly higher molecular weight of poly(EDTT)-E. However, neither poly(EDTT)-C nor poly(EDTT)-E are optically transparent in the doped state, as has been claimed for the oxygen analog PEDT.¹⁴

Photoluminescence Spectroscopy. The photoluminescence spectra of the polymers were studied both in solution and in the solid state. Figure 9A shows the emission spectra of both poly(EDTT)-C and poly(EDTT)-E in dilute NMP solution (~ 1 mg/30 mL) at room temperature when excited at 400 nm. Photoexcitation of these polymers results in broad band luminescence with a peak at ca. 552 nm (2.25 eV), and half-height width of 0.33 eV for both poly(EDTT)-C and poly(EDTT)-E. Both emission spectra exhibit a broad tail at low energy, presumably a result of emission from longer conjugated segments.²⁶ Figure 9B shows the excitation spectra of the poly(EDTT)-C and poly(EDTT)-E in dilute NMP solution at room temperature with emission monitored at 552 nm. Both spectra show two peaks at ca. 340 and 394 nm, which correspond to the two absorptions in the UV-vis spectra (Figure 7). In the solid state, the poly(EDTT)-C emits light at low energy (at 611 nm) when excited at 350 nm (see Figure

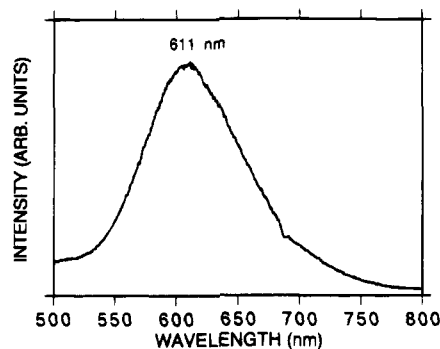


Figure 10. Fluorescence emission spectra of poly(EDTT)-C in the solid state at room temperature ($\lambda_{\text{ex}} = 350$ nm).

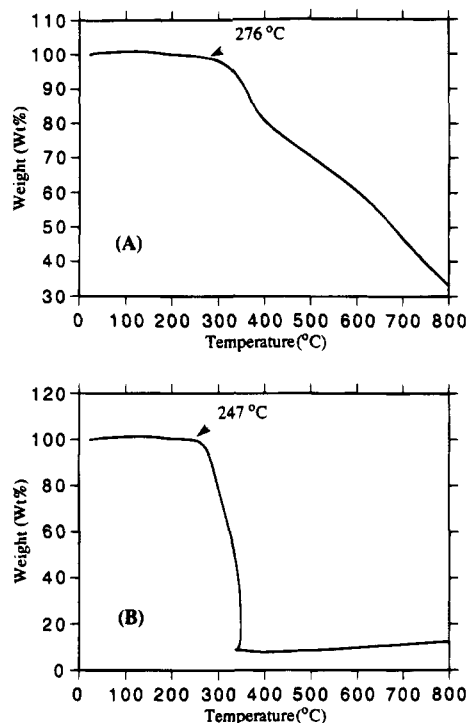


Figure 11. TGA thermograms of neutral poly(EDTT)-C (A) under nitrogen and (B) under oxygen.

10). This is in good agreement with the decrease in bandgap observed in going from solution to the solid state. The photoluminescence data suggest that these materials may be good candidates for application in electroluminescence devices.

Thermal Analysis. The thermal properties of the neutral poly(EDTT)-C were examined by thermogravimetric analysis (TGA), and the results are depicted in Figure 11. The poly(EDTT)-C under nitrogen atmosphere starts to decompose at 276 °C and loses about 66% of its weight by 800 °C. The decomposition in oxygen starts at ~ 245 °C and results in 92% weight loss by 400 °C. By comparison, poly(3-octylthiophene) exhibits thermal stability in nitrogen up to 300 °C and about 250 °C in oxygen.²⁷

Figure 12 shows the DSC thermogram of poly(EDTT)-C under nitrogen atmosphere. At the first heating and cooling cycle it displays an irreversible sharp exothermic peak at ca. 253 °C with the heating and cooling rate of 5 °C/min. The exothermic peak is an irreversible event and could be due to energy

(25) Patil, A. O.; Heeger, A. J.; Wudl, F. *Chem. Rev.* **1988**, *88*, 183–200.

(26) Xu, B.; Holdcroft, S. *J. Am. Chem. Soc.* **1993**, *115*, 8447–8448.

(27) Gustafsson, G.; Inganäs, O.; Nilsson, J. O. *Synth. Met.* **1989**, *28*, C435–C444.

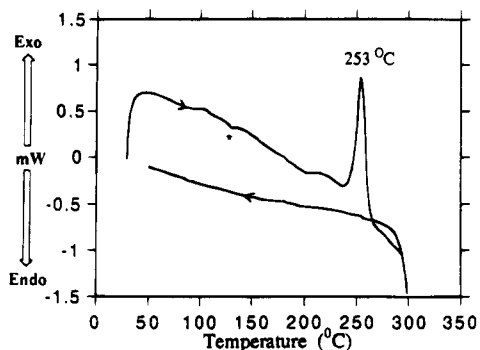


Figure 12. DSC thermogram of neutral poly(EDTT)-C (under nitrogen) (* due to the baseline of empty Al pan).

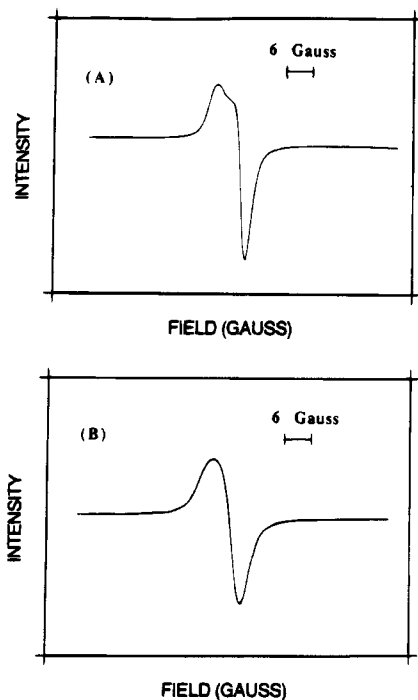


Figure 13. ESR spectra of neutral poly(EDTT)-C (A) at 23 °C and (B) -157 °C.

released from ring opening of the fused ring substituted on the thiophene.

Electron Spin Resonance Spectroscopy. The nature of localized and itinerant spins in the poly(EDTT) materials was probed by ESR spectroscopy. Figure 13 shows the ESR spectrum of the neutral poly(EDTT)-C at room temperature (RT) of 23 °C and low temperature (LT) of -157 °C. A largely anisotropic signal with g values of 2.0062 (g_1) and 2.0035 (g_2) was well resolved at 23 °C, while it was less resolved at -157 °C. The number of spins corresponding to this signal was calculated (using a DPPH standard) to be $\sim 5.89 \times 10^{20}$ spins/mol and $\sim 3.40 \times 10^{20}$ spins/mol for the room-temperature and low-temperature measurements, respectively. The origin of these spins lies in defects along the polymer backbone. At room temperature there is approximately 1 spin per ~ 1022 rings (corresponding to a bulk susceptibility of $\chi_m = 1.2 \times 10^{-6}$ emu/mol), which is a very small number compared to other conjugated polymers and indicative of a high-quality polymer.

In contrast to the generally observed single symmetrical line of poly(alkylthiophenes),^{3a,28} the larger g_1 and anisotropic character of the ESR spectra of the neutral poly(EDTT)-C indicates that the orbitals of the

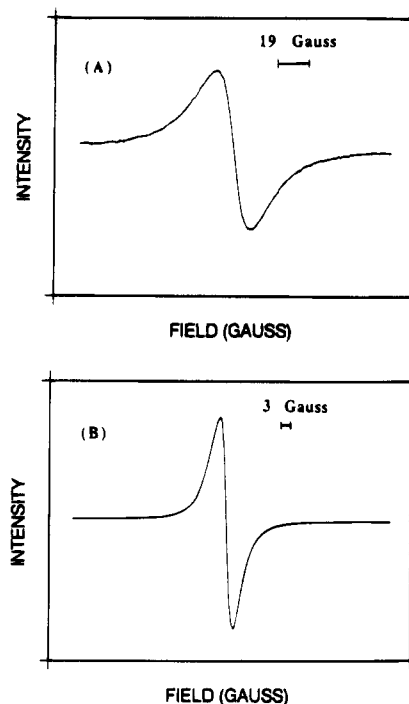


Figure 14. ESR spectra of (A) doped poly(EDTT)-C (I_3^-) and (B) doped poly(EDTT)-E (ClO_4^-) at 23 °C.

sulfur atoms in the thiophene ring periphery are significantly involved in the highest occupied molecular orbital (HOMO) of the polymer where the unpaired spins reside. It appears that the spins localize part of the time on the ethanedithiolate sulfur atoms, instead of just along the conjugated backbone, which would imply a significant degree of mixing of the 3s and 3p orbitals on the sulfur atoms with the thiophene carbon p orbitals as has been proposed in the related PEMT and PBEMT.¹³

The anisotropic ESR spectrum becomes more symmetric and more intense when poly(EDTT)-C is iodine doped, see Figure 14. The broad nearly symmetrical line ($\Delta H_{pp} \sim 19$ G) at $g = 2.0058$ at 23 °C, corresponds to $\sim 1.16 \times 10^{21}$ spins/mol. At -157 °C, the line width of the ESR spectrum decreases to 7.2 G at $g = 2.0061$. The dramatic changes of the ESR line shapes and intensities in going from the neutral to the doped state of poly(EDTT)-C are attributed to the significant changes in electronic structure, the increase in the number of defects in the polymer backbone during the doping process, and perhaps the appearance of some itinerant spins. The contribution of the ethane-dithiolate ring substituent to the ESR response is less significant in the doped poly(EDTT)-C, possibly due to either the greater delocalization of spins in the oxidized, conducting, state or the formation of the bipolaron band which contains virtually no contributions from the substituted sulfur orbitals in the fused six-membered ring. The creation of additional spins whose spectrum masks that of those present in the undoped material cannot be ruled out.

The ESR spectra of neutral and doped (ClO_4^-) poly(EDTT)-E reveal similar features as the neutral and doped poly(EDTT)-E at 23 and -157 °C, i.e., anisotropic and isotropic line shape for the neutral and doped

Table 2. ESR Data for Various Poly(EDTT) Samples

sample	<i>g</i> factor	ΔH_{pp} (G)	spins/mol	line shape
At 23 °C				
poly(EDTT)-C (neutral)	2.0062	6.0	5.89×10^{20}	anisotropic
	2.0035			
poly(EDTT)-E (neutral)	2.0062	6.0	4.64×10^{21}	anisotropic
	2.0035			
poly(EDTT)-C (I ₃ ⁻ doped)	2.0058	19.3	1.16×10^{21}	isotropic
poly(EDTT)-E (ClO ₄ ⁻ doped)	2.0047	3.2	8.36×10^{21}	isotropic
At -157 °C				
poly(EDTT)-C (neutral)	2.0059	6.0	3.40×10^{20}	anisotropic
	2.0035			
poly(EDTT)-E (neutral)	2.0060	6.0	3.39×10^{21}	anisotropic
	2.0035			
poly(EDTT)-C (I ₃ ⁻ doped)	2.0061	7.2	1.21×10^{21}	isotropic
poly(EDTT)-E (ClO ₄ ⁻ doped)	2.0046	2.8	1.31×10^{22}	isotropic

polymer, respectively. The detailed ESR data for all versions of poly(EDTT) are summarized in Table 2.

Charge-Transport Properties. *Electrical Conductivity.* The electrical conductivities of doped poly(EDTT)-C (with FeCl₄⁻) and doped poly(EDTT)-E (with ClO₄⁻) and also the neutral materials were measured by the standard four-probe method on pressed pellets as a function of temperature. In the neutral state, the polymers have conductivities $\sim 10^{-10}$ S/cm at room temperature. With doping, the room-temperature conductivities increase to ~ 0.1 S/cm for poly(EDTT)-C and 0.4 S/cm for poly(EDTT)-E. These samples maintain these conductivities for several months. These conductivity values are comparable to that of the poly(DBTT) and among the highest obtained in mercapto-substituted polythiophenes. They are several orders of magnitude higher than those of the related polymer PBEMT ($\sigma = 10^{-7}$ S/cm) and PEMT ($\sigma = 10^{-3}$ S/cm)¹³ and about 2 orders of magnitude lower than that of PEDT ($\sigma = 15\text{--}19$ S/cm).¹⁴ The slightly higher conductivity of poly(EDTT)-E compared to poly(EDTT)-C is in good agreement with its higher molecular weight. Given the comparable molecular weights of PBEMT, PEMT, poly(EDTT)-C, and poly(EDTT)-E, one reason for the high conductivity of the latter two polymers is that their charge carriers are less localized on the peripheral sulfur atoms compared to PEMT and PBEMT,¹³ which could give rise to higher carrier mobilities. A contributing factor may be the decreased steric interactions in poly(EDTT) due to the cyclic disubstitution pattern on the thiophene ring which eliminates α,β couplings and gives rise to a more planar backbone.

The electrical conductivity of poly(EDTT)-C and poly(EDTT)-E was also measured as a function of temperature and shows a thermally activated behavior in which the conductivity drops with falling temperature. The data in Figure 15 show that the temperature dependence does not follow the typical semiconductor behavior for a single activation energy. This suggests that the charge transport in these materials is affected by scattering mechanisms that are not dominant in classical semiconductor samples. A significant factor affecting charge flow in these samples is boundaries between adjacent polymer grains as well as other activation barriers associated with chain-to-chain transport. To gain further insight into the conduction mechanism of poly(EDTT)-C and poly(EDTT)-E, we attempted to fit the experimental variable temperature data to the analytical expression

$$\sigma = \sigma_0 \exp[-(T_0/T)^\alpha]$$

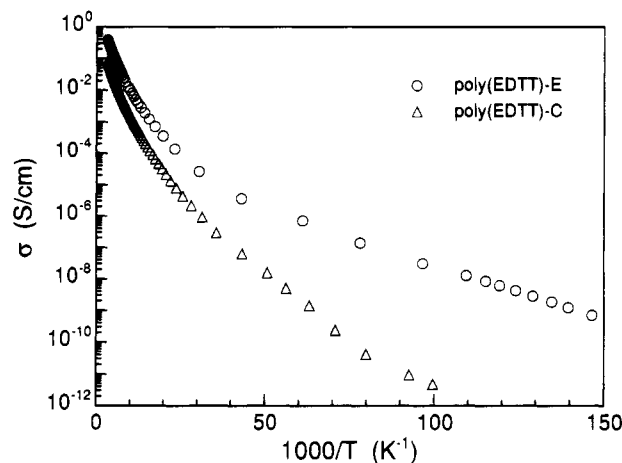


Figure 15. Four-probe variable-temperature electrical conductivity of (A) poly(EDTT)-C doped with FeCl₄⁻ and (B) poly(EDTT)-E doped with ClO₄⁻. The temperature range is 5–300 K.

where σ_0 and T_0 are constants and $\alpha = 1/2, 1/3,$ or $1/4$ based on several conduction mechanisms suggested for such systems.^{29,30} It must be noted that several conduction models, such as carrier tunneling between small metallic particles in an insulating matrix,^{29,30} one-dimensional variable range hopping (1D-VRH) between localized states,³⁰ and the Coulomb gap model for certain disordered systems³¹ can be described with $\alpha = 1/2$. Three-dimensional variable range hopping (3D-VRH) is described by $\alpha = 1/4$. Single-exponential fits of the electrical conductivity data, with $\alpha = 1/2$ and $\alpha = 1/4$, are shown in Figure 16. It is clear from these plots that the fits over the entire temperature range are not entirely satisfactory except for poly(EDTT)-C when $\alpha = 1/2$, which excludes the 3D-VRH model for this material. The poly(EDTT)-E shows a definite change in slope at 25 K below which it gives a good fit for $\alpha = 1/2$. This slope change may be due to a change in charge-transport mechanism. In any case it would be difficult to separate the effect of grain boundaries from that of interchain hopping with the data at hand. Given the one-dimensional nature of the conducting species in these polymers it is reasonable to envision a charge-transport model favoring a 1D-VRH.

(29) (a) Abeles, B.; Sheng, P.; Coutts, M. D.; Arie, Y. *Adv. Phys.* **1975**, *24*, 407–461. (b) Sheng, P. *Phys. Rev. B: Condens. Matter* **1980**, *B21*, 2180–2195. (c) Sheng, P.; Abeles, B.; Arie, Y. *Phys. Rev. Lett.* **1973**, *31*, 44–47.

(30) Isotalo, H.; Stubb, H.; Yli-Lahti, P.; Kuivalainen, P.; Österholm, J.-E.; Laasko, J. *Synth. Met.* **1989**, *28*, C461–C466.

(31) Efros, A. L.; Shklovskii J. *Phys. C: Solid State Phys.* **1975**, *C8*, L49–L51.

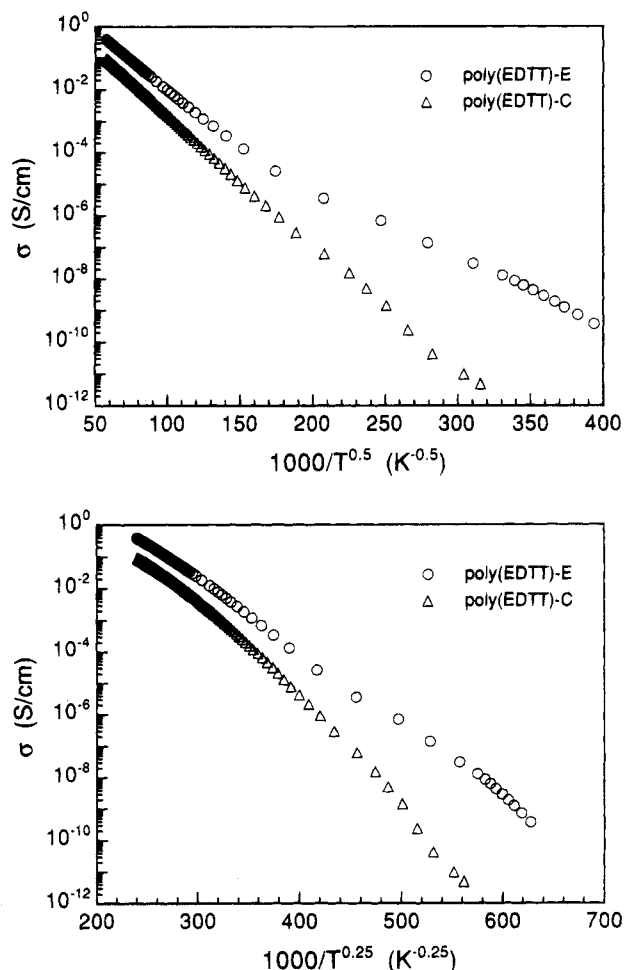


Figure 16. Four-probe variable-temperature electrical conductivity of poly(EDTT)-C, doped with FeCl_4^- and poly(EDTT)-E, doped with ClO_4^- : (top) $\log \sigma$ vs $T^{-1/2}$ format; (bottom) $\log \sigma$ vs $T^{-1/4}$ format. The temperature range is 5–300 K.

Thermoelectric power measurements are less susceptible to grain boundary effects and can better probe the intrinsic transport properties of materials. That is because it is a zero-current technique. Such measurements were performed on doped pressed pellets of both the chemically and electrochemically derived polymer. The values of the thermopower varied from -5 to $+5$ $\mu\text{V/K}$ and in all samples this property trended toward zero at lower temperatures; see Figure 17. The magnitude of the thermopower suggests a metallic state for doped poly(EDTT) as has been found in other highly conducting polythiophenes. The vacillation between a negative and a positive sign to the thermopower, in what appears to be similarly doped samples, is more difficult to assess. Ideally, oxidatively doped poly(EDTT) should be a p-type conductor if the polaron/bipolaron model proposed for these materials is correct. All other polythiophene derivatives have found to possess small positive thermopowers between 300 and 5 K.¹⁰ Although such changes in thermopower sign have

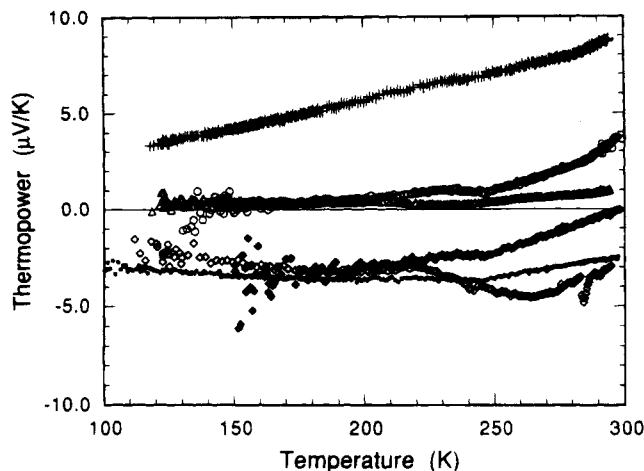


Figure 17. Variable-temperature thermopower data for several pressed pellet samples of doped poly(EDTT). Regardless of chemical or electrochemical origin of the sample, both positive and negative thermopower values have been observed.

been previously observed in polyaniline samples, they have been attributed to variations in protonation levels. This possibility does not exist in poly(EDTT), and thus a satisfactory explanation cannot be advanced at this state. The findings reported here with respect to the thermopower of poly(EDTT) may imply that currently accepted views of charge transport in some conjugated polymers may need further refinement. Work to identify the factors that affect the sign of the thermopower from sample to sample is continuing.

Concluding Remarks

The incorporation of the ethylenedimercapto group at the 3,4-positions of thiophene allows for a better control of polymer synthesis and gives the resultant polymer high solubility, unusual optical absorption, and anisotropic ESR spectra. In contrast to its oxygen analog, PEDT, poly(EDTT) is not optically transparent in the doped state. The doped polymer shows metallic conductivity with $\sigma \sim 0.1$ – 0.4 S/cm at room temperature about 2–6 orders of magnitude higher than that of PEMT and PBEMT, two polythiophenes with mercapto substituents on the thiophene ring. The dramatic enhancements in the conductivity of poly(EDTT) can be attributed to improved conjugation and better inter-chain contacts compared to other poly(mercaptothiophenes). We note, however, that these conductivity values are still much lower than those claimed for PEDT. The reasons for this difference are not clear.

Acknowledgment. Financial support from the National Science Foundation (DMR-93-06385) is gratefully acknowledged. At Northwestern University this work made use of Central Facilities supported by the NSF through the Materials Research Center (DMR-91-20521). We thank Professor Eugene LeGoff for fruitful discussions.